Nonlinear Inelastic Analysis of Space Steel Structures

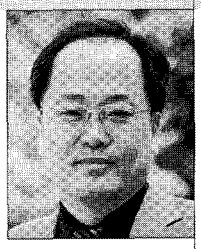

Huu-Tai Thai* 김 승 억**

*세종대학교 토목환경공학과 박사과정
**세종대학교 토목환경공학과 교수

1. Introduction

It is widely recognized that steel structures may exhibit significantly nonlinear behavior prior to achieving their ultimate load-carrying capacity. Thus, a nonlinear inelastic analysis or advanced analysis is the most rational mean for assessment of the performance of a whole structural system instead of using conventional analysis/design approach. Advanced analysis indicates any analysis methods which can capture strength and behavior of a structural system and its component members without requiring the separate member capacity checks(Thai and Kim, 2009). In general, advanced analysis can be classified into two categories of plastic zone and plastic hinge types. In the plastic zone, the beam-column member is divided into many finite elements and the cross-section of each element is further subdivided into many fibers of which the uniaxial stress-strain relationships of material are monitored during the analysis process. Although the solution of this method can be considered to be accurate, it is too computationally intensive because a very refined discretisation of the structure is required. In the plastic hinge, the beam-column member is modeled by an appropriate way to eliminate its further subdivision. The inelastic behavior of material is assumed to be lumped at both ends of the member. The main merits of this method are that it is simple in formulation as well as implementation and, more importantly, the least element is required to model the member.

The purpose of this paper is to develop a structural analysis program which can capture accurately and efficiently the strength and behavior of three-dimensional steel structures comprising of truss, beam-column, and cable members subjected to static and dynamic loadings. The proposed program can be used to assess realistically both strength and behavior of a structural system and its component members in a direct manner. Three nonlinear elements considering both geometric and material nonlinearities are implemented into a computer program: (1) cable element; (2) truss element; and (2) beam-column element. Three types of analysis provided in the proposed program are: (1) linear and nonlinear static analysis; (2) linear and nonlinear time-history analysis; and (3) free vibration analysis. In static analysis, generalized displacement control algorithm proposed by Yang and Shieh(1990) is adopted for solving the nonlinear equilibrium equations because of its numerical stability and efficiency. This algorithm can trace the equilibrium paths of nonlinear problems with multiple limit points and snap-back

points. In time-history analysis, an incremental-iterative scheme based on the Newmark-β and Newton-Raphson method is adopted for solving the nonlinear equations of motion. Several numerical examples are presented to verify the accuracy and efficiency of the proposed program. The predictions are compared with those obtained using commercial package of ABAQUS and SAP2000, and the other results reported in the literature.

2. Formulation

2.1 Cable element

The sag effects of cable due to its self-weight and pretension can be captured accurately using the catenary cable element, while the inelastic behavior of cable is represented by an elastic-plastic hinge model. The tangent stiffness matrix of a three-dimensional cable element is derived based on exact analytical expressions of elastic catenary as follows

$$K_T = \begin{bmatrix} -K & K \\ K & -K \end{bmatrix} \tag{1}$$

where

$$K = F^{-1} = \begin{bmatrix} f_{11} & f_{12} & f_{13} \\ f_{12} & f_{22} & f_{23} \\ f_{13} & f_{23} & f_{33} \end{bmatrix}^{-1} \tag{2}$$

in which

$$f_{11} = -\left(\frac{L_0}{EA} + \frac{1}{w}\log\frac{T_j + F_6}{T_i - F_3}\right) + \frac{F_1^2}{w}\left[\frac{1}{T_i(T_i - F_3)} - \frac{1}{T_j(T_j + F_6)}\right]$$

$$f_{12} = \frac{F_1 F_2}{w}\left[\frac{1}{T_i(T_i - F_3)} - \frac{1}{T_j(T_j + F_6)}\right], \quad f_{13} = \frac{F_1}{w}\left[\frac{1}{T_j} - \frac{1}{T_i}\right]$$

$$f_{22} = -\left(\frac{L_0}{EA} + \frac{1}{w}\log\frac{T_j + F_6}{T_i - F_3}\right) + \frac{F_2^2}{w}\left[\frac{1}{T_i(T_i - F_3)} - \frac{1}{T_j(T_j + F_6)}\right]$$

$$f_{23} = \frac{F_2}{w}\left[\frac{1}{T_j} - \frac{1}{T_i}\right], \quad f_{33} = -\frac{L_0}{EA} - \frac{1}{w}\left[\frac{F_6}{T_j} + \frac{F_3}{T_i}\right]$$

$$F_4 = -F_1,\ F_5 = -F_2,\ F_6 = -F_3 + wL_0,\ T_i = \sqrt{F_1^2 + F_2^2 + F_3^2},\ T_j = \sqrt{F_4^2 + F_5^2 + F_6^2} \tag{3}$$

where E is the elastic modulus; A is the cross-sectional area; L_o is the unstressed length; w is the self-weight per unit length of cable; F_1, F_2, F_3 and F_4, F_5, F_6 are the global nodal force at node i and j, respectively; T_i and T_j are cable tensions at node i and j.

2.2 Truss element

The incremental form of equilibrium equations for the space truss element can be derived based on the principle of virtual displacement as

$$\left([k_E] + [k_G] + [s_1] + [s_2] + [s_3]\right)\{d\} + {}^1f = {}^2f \tag{4}$$

where $[k_E]$ and $[k_G]$ are the elastic and geometric stiffness matrices, respectively; $[s_1]$, $[s_2]$ and $[s_3]$ are higher-order stiffness matrices given in Yang and Kou(1994); ${}^1f$ is the initial nodal forces acting on the element at C_1 ; ${}^2f$ and is the total nodal forces acting on the element at C_2.

The material nonlinearity is accounted for by tracing a simple empirical equation of stress-strain relationship proposed by Hill et al.(1989). The stress-strain curve is expressed by the following equations:

For tensile members

$$\sigma = E\varepsilon, \quad \varepsilon < \varepsilon_y \tag{5a}$$

$$\sigma = \sigma_y, \quad \varepsilon \geq \varepsilon_y \tag{5b}$$

For compressive members

$$\sigma = E\varepsilon, \quad |\varepsilon| < |\varepsilon_{cr}| \tag{6a}$$

$$\sigma = \sigma_{cr}, \quad |\varepsilon_{cr}| \leq |\varepsilon| < |\varepsilon_0| \tag{6b}$$

$$\sigma = \sigma_l + (\sigma_{cr} - \sigma_l)\exp\left[-\left(X_1 + X_2\sqrt{\varepsilon'}\right)\varepsilon'\right], \quad |\varepsilon| \geq |\varepsilon_0| \tag{6c}$$

where σ_y and ε_y are the yield stress and corresponding yield strain, respectively; X_1 and X_2 are the constants based on the slenderness ratio (L/r) of the compressive members; σ_l is the asymptotic lower stress limit; ε' is the axial strain measured from the beginning of inelastic post-buckling range; σ_{cr} and ε_{cr} are the Euler critical buckling stress and corresponding critical buckling strain, respectively.

2.3 Beam-column element

To minimize the modeling and solution time, the stability function is employed to capture the geometric nonlinearities, and the refined plastic hinge model is adopted to represent

the material nonlinearities. Although the formulations of the beam-column element have been discussed in detail by authors in a previous paper(Thai and Kim, 2009), a brief discussion is also presented in this paper for the sake of completeness.

2.3.1 Stability functions accounting for second-order effects

The incremental form of member basic force and deformation relationship of space beam-column element can be expressed as

$$\begin{Bmatrix} P \\ M_{yA} \\ M_{yB} \\ M_{zA} \\ M_{zB} \end{Bmatrix} = \begin{bmatrix} EA/L & 0 & 0 & 0 & 0 \\ 0 & S_1EI_y/L & S_2EI_y/L & 0 & 0 \\ 0 & S_2EI_y/L & S_1EI_y/L & 0 & 0 \\ 0 & 0 & 0 & S_3EI_z/L & S_4EI_z/L \\ 0 & 0 & 0 & S_4EI_z/L & S_3EI_z/L \end{bmatrix} \begin{Bmatrix} \delta \\ \theta_{yA} \\ \theta_{yB} \\ \theta_{zA} \\ \theta_{zB} \end{Bmatrix} \tag{7}$$

where P, M_{yA}, M_{yB}, M_{zA} and M_{zB} are incremental axial force and end moments with respect to y and z axes; δ, θ_{yA}, θ_{yB}, θ_{zA} and θ_{zB} are the incremental axial displacement and joint rotations; S_1, S_2, S_3 and S_4 are the stability functions with respect to y and z axes. It should be noted that the Hermite cubic interpolation function is a specific case of stability function when the axial force is equal to zero.

2.3.2 Refined plastic hinge model accounting for inelastic effects

The gradual yielding due to residual stresses is considered by utilizing the Column Research Council(CRC) tangent modulus concept E_t, while the gradual yielding due to flexure is represented by the parabolic functions η. The relationship between basic force and deformation of space beam-column accounting for the inelastic effects is modified as

$$\begin{Bmatrix} P \\ M_{yA} \\ M_{yB} \\ M_{zA} \\ M_{zB} \end{Bmatrix} = \begin{bmatrix} E_tA/L & 0 & 0 & 0 & 0 \\ 0 & k_{iiy} & k_{ijy} & 0 & 0 \\ 0 & k_{ijy} & k_{jjy} & 0 & 0 \\ 0 & 0 & 0 & k_{iiz} & k_{ijz} \\ 0 & 0 & 0 & k_{ijz} & k_{jjz} \end{bmatrix} \begin{Bmatrix} \delta \\ \theta_{yA} \\ \theta_{yB} \\ \theta_{zA} \\ \theta_{zB} \end{Bmatrix} \tag{8}$$

where

$$k_{iiy} = \eta_A\left(S_1 - \frac{S_2^2}{S_1}(1-\eta_B)\right)\frac{E_tI_y}{L} \tag{9a}$$

$$k_{ijy} = \eta_A\eta_B S_2 \frac{E_tI_y}{L} \tag{9b}$$

$$k_{jjy} = \eta_B\left(S_1 - \frac{S_2^2}{S_1}(1-\eta_A)\right)\frac{E_tI_y}{L} \tag{9c}$$

$$k_{iiz} = \eta_A\left(S_3 - \frac{S_4^2}{S_3}(1-\eta_B)\right)\frac{E_tI_z}{L} \tag{9d}$$

$$k_{ijz} = \eta_A\eta_B S_4 \frac{E_tI_z}{L} \tag{9e}$$

$$k_{jjz} = \eta_B\left(S_3 - \frac{S_4^2}{S_3}(1-\eta_A)\right)\frac{E_tI_z}{L} \tag{9f}$$

The terms and η_A are η_B scalar parameters that allow for gradual inelastic stiffness reduction of the element associated with plastification at ends A and B. These terms are equal to 1.0 when the element is elastic, and zero when a plastic hinge is formed. The parameter η is assumed to vary according to the parabolic function as

$$\eta = 1.0 \quad \text{for} \quad \alpha \le 0.5 \tag{10a}$$

$$\eta = 4\alpha(1-\alpha) \quad \text{for} \quad \alpha > 0.5 \tag{10b}$$

where can be expressed in the Orbison yield surfaces as

$$\alpha = 1.15p^2 + m_z^2 + m_y^4 + 3.67p^2m_z^2 + 3.0p^6m_y^2 + 4.65m_z^4m_y^2 \tag{11}$$

where $p=P/P$, $m_z=M_z/M_{pz}$(strong-axis), $m_y=M_y/M_{py}$(weak-axis).

3. Solution algorithm

3.1 Solution algorithm for static analysis

Among several solution methods which can trace the equilibrium path of problem with multiple limit points and snap-back points, the generalized displacement control algorithm appears to be the most robust and effective method because of its numerical stability and efficiency. Therefore, it is adopted herein for static analysis. The incremental equilibrium equation of structure can be rewritten for the th iteration of the th incremental step as

$$\left[K_{j-1}^i\right]\left\{\Delta D_j^i\right\} = \lambda_j^i\left\{\hat{P}\right\} + \left\{R_{j-1}^i\right\} \tag{12}$$

where $[K_{j-1}^i]$ is the tangent stiffness matrix, $\{\Delta D_j^i\}$ is the displacement increment vector, $\{\hat{P}\}$ is the reference load vector, $\{R_{j-1}^i\}$ is the unbalanced force vector, and λ_j^i is the load increment parameter.

For convenience, Eq. (12) can be decomposed into the

following equations:

$$\left[K_{j-1}^{i}\right]\left\{\Delta\hat{D}_{j}^{i}\right\}=\left\{\hat{P}\right\} \tag{13}$$

$$\left[K_{j-1}^{i}\right]\left\{\Delta\bar{D}_{j}^{i}\right\}=\left\{R_{j-1}^{i}\right\} \tag{14}$$

$$\left\{\Delta D_{j}^{i}\right\}=\lambda_{j}^{i}\left\{\Delta\hat{D}_{j}^{i}\right\}+\left\{\Delta\bar{D}_{j}^{i}\right\} \tag{15}$$

The load increment parameter λ_j^i is determined from a constraint condition. For the first iterative step (j=1), the load increment parameter λ_j^i is determined based on the Generalized Stiffness Parameter (*GSP*) as

$$\lambda_1^i=\lambda_1^1\sqrt{|GSP|} \tag{16}$$

where λ_1^1 is an initial value of load increment parameter, and the *GSP* is defined as

$$GSP=\frac{\left\{\Delta\hat{D}_{1}^{1}\right\}^{T}\left\{\Delta\hat{D}_{1}^{1}\right\}}{\left\{\Delta\hat{D}_{1}^{i-1}\right\}^{T}\left\{\Delta\hat{D}_{1}^{i}\right\}} \tag{17}$$

For the iterative step ($j\geq2$), the load increment parameter λ_j^i is calculated as

$$\lambda_{j}^{i}=-\frac{\left\{\Delta\hat{D}_{1}^{i-1}\right\}^{T}\left\{\Delta\bar{D}_{j}^{i}\right\}}{\left\{\Delta\hat{D}_{1}^{i-1}\right\}^{T}\left\{\Delta\hat{D}_{j}^{i}\right\}} \tag{18}$$

where $\{\triangle\widehat{D_j^i}\}$ is the displacement increment generated by reference load $\{\hat{P}\}$ at the first iteration of previous incremental step (i-1). $\{\triangle\widehat{D_j^i}\}$ and $\{\triangle\overline{D_j^i}\}$ denote the displacement increments generated by the reference load and unbalanced force vectors, respectively, at the jth iteration of the ith incremental step, as defined in Eqs. (13) and (14).

3.2 Solution algorithm for dynamic analysis

The incremental equation of motion of a structure can be written as

$$[M]\{\Delta\ddot{D}\}+[C]\{\Delta\dot{D}\}+[K]\{\Delta D\}=\{\Delta F\} \tag{19}$$

where $[\triangle\ddot{D}]$, $[\triangle\dot{D}]$, and $[\triangle D]$ are the vectors of incremental acceleration, velocity, and displacement, respectively; $[M]$, $[C]$, and $[K]$ are the mass, damping, and tangent stiffness matrices, respectively; $\{\triangle F\}$ is the external load increment vector.

Adopting the average acceleration method of the Newmark family (γ=1/2, β=1/4), the incremental equation of motion can be written as

$$\left[\hat{K}\right]\{\Delta D\}=\left\{\Delta\hat{F}\right\} \tag{20}$$

where $[\hat{K}]$ and $[\triangle\hat{F}]$ are the effective stiffness matrix and incrementally effective force vector, respectively, given as

$$\left[\hat{K}\right]=\frac{4}{\Delta t^{2}}[M]+\frac{2}{\Delta t}[C]+[K] \tag{21}$$

$$\left\{\Delta\hat{F}\right\}=\{\Delta F\}+\left\{\frac{4}{\Delta t}[M]+2[C]\right\}\left\{\dot{D}_{n}\right\}+2[M]\left\{\ddot{D}_{n}\right\} \tag{22}$$

For the second and subsequent iterations of each time step, the structural system is solved under the effect of the unbalanced force $\{\triangle R\}$ as

$$\left[\hat{K}\right]\{\Delta\Delta D\}=\{\Delta R\} \tag{23}$$

where the unbalanced force $\{\triangle R\}$ is determined based on the total external force , inertial force, damping force, and updated internal force $\{F_{\text{int}}\}$ as

$$\{\Delta R\}=\{F_{n+1}\}-[M]\left\{\ddot{D}_{n+1}\right\}-[C]\left\{\dot{D}_{n+1}\right\}-\{F_{\text{int}}\} \tag{24}$$

Once the convergence criterion is satisfied, the structural response is updated for the next time step as

$$\left\{\Delta D^{k+1}\right\}=\left\{\Delta D^{k}\right\}+\{\Delta\Delta D\} \tag{25}$$

$$\left\{D_{n+1}\right\}=\left\{D_{n}\right\}+\left\{\Delta D^{k+1}\right\} \tag{26}$$

$$\left\{\dot{D}_{n+1}\right\}=-\left\{\dot{D}_{n}\right\}+\frac{2}{\Delta t}\left\{\Delta D^{k+1}\right\} \tag{27}$$

$$\left\{\ddot{D}_{n+1}\right\}=-\left\{\ddot{D}_{n}\right\}-\frac{4}{\Delta t}\left\{\dot{D}_{n}\right\}+\frac{4}{\Delta t^{2}}\left\{\Delta D^{k+1}\right\} \tag{28}$$

4. Verification study

The proposed software is verified for the accuracy and computational efficiency through several numerical examples under static and dynamic loadings. The El Centro earthquake with peak ground acceleration of 0.319g(g=9.81m/s^2) is used. In the time-history analysis, the mass-and stiffness-proportional damping factors are chosen based on the first two modes of structures so that the equivalent viscous damping ratio is equal to 5%.

4.1 Plane cable under static and dynamic loadings

The first example is a plane cable subjected to static and dynamic loadings as shown in Fig. 1. The static loading is applied at all internal nodes of the cable, while the earthquake loading is assumed to be applied in the vertical direction. It should be noted that the cable element provided by SAP2000 ignores the inelastic behavior.

The obtained static displacements are compared with those predicted by SAP2000 as shown in Table 1. It can be seen that a good agreement is obtained.

The displacement responses of the cable subjected to both static and El Centro earthquake loadings obtained by the proposed program and SAP2000 are compared in Fig. 2. It can be seen that all results are in a good agreement. This one also indicates that the cable element in the proposed program can accurately predict the seismic response of cable structures. To investigate the inelastic effect of seismic response of the cable net, the inelastic time-history analysis is carried out using the proposed program because the cable element provided by SAP2000 can not consider the inelastic behavior. The inelastic responses of the plane cable obtained by the proposed program are shown in Fig. 2. It can be seen that the inelastic response is significant discrepancies compared to the elastic response.

Table 1 Comparison of displacements of plane cable under static loading

Software	Displacements of node 4(mm)		
	x-direction	y-direction	z-direction
SAP2000	-40.28	-40.28	-448.88
Present	-40.13	-40.13	-446.50

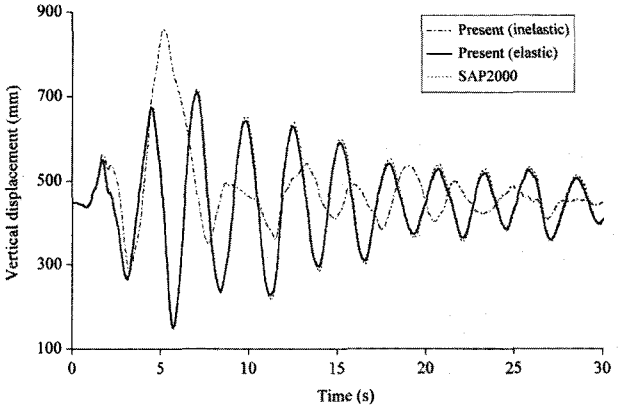

Fig. 2 Displacement responses at node 4 of the plane cable under El Centro

4.2 Star dome truss under static loading

Fig. 3 shows a 24-member star dome truss subjected to a concentrated load P at the center. This structure was analyzed previously by Hill et al.(1989) using the arc-length method. Each member of the truss has an area of $10mm^2$ and weak axis moment of inertia of $41.7mm^4$. The elastic modulus and yield stress of the material are 203.4*GPa* and 400*MPa*, respectively. Three different cases of elastic, elastic post-buckling(EPB) and inelastic post-buckling(IPB) analyses have been performed using the following parameters of Hill model: X_1=50; X_2=100; σ_1=0.4σ_{cr}; ε_0=ε_{cr}.

The load-displacement curves at the center of the truss predicted by the proposed program and Hill are compared in Fig. 4. It can be seen that the results obtained by the proposed program agree well with those generated by Hill in three analysis cases of elastic, EPB and IPB. The limit load obtained in the proposed program from elastic analysis is 641.66 N compared to 658.72 N given by Hill, while the limit load from EPB and

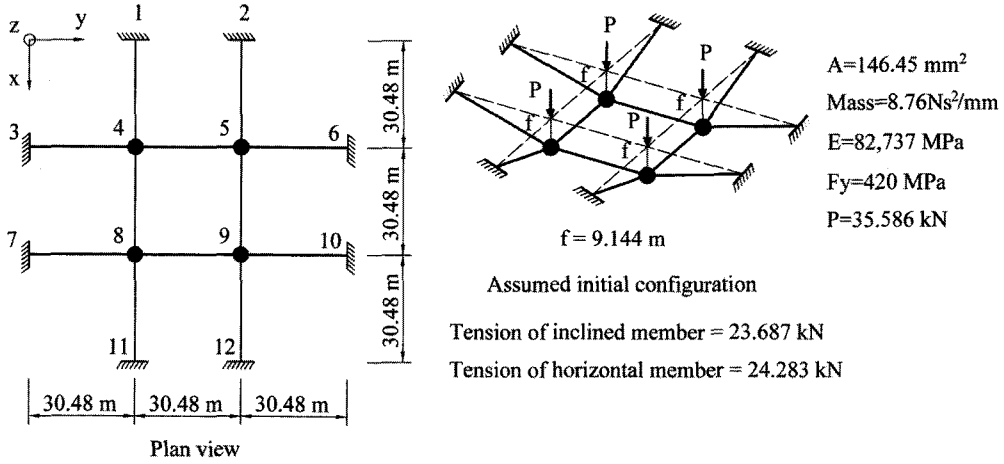

Fig. 1 Plane cable under static and dynamic loadings

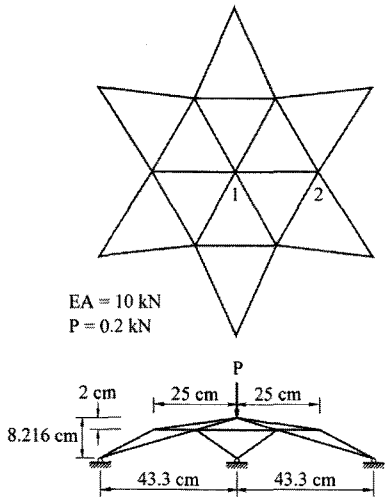

Fig. 3 Star dome truss

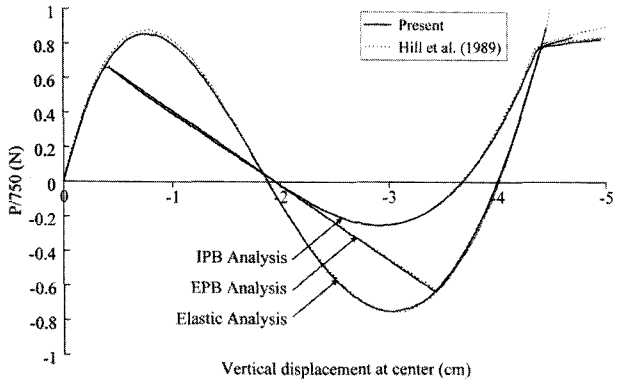

Fig. 4 Load-displacement curves of star dome truss at center

IBP analyses of the proposed program is 493.60 N which is identical with that given by Hill.

4.3 Space truss under earthquake loading

A 72-member space truss taken from Heidari and Salajegheh (2006) is used to show the capability of the proposed program in predicting the nonlinear inelastic seismic responses of large-scale truss structure. The geometric dimension of the space truss is kept to be the same with the original one, but the original cross-section and the original masses of the structure are changed to be capable of showing inelastic and inelastic buckling behavior clearly under earthquake excitations. Geometry, mass distribution, and material properties of the modified truss are shown in Fig. 5.

The displacement responses of the truss obtained by the proposed program and ABAQUS are compared in Fig. 6. It can be seen that all results are in a very good agreement including the permanent shifts in displacement due to inelastic behavior.

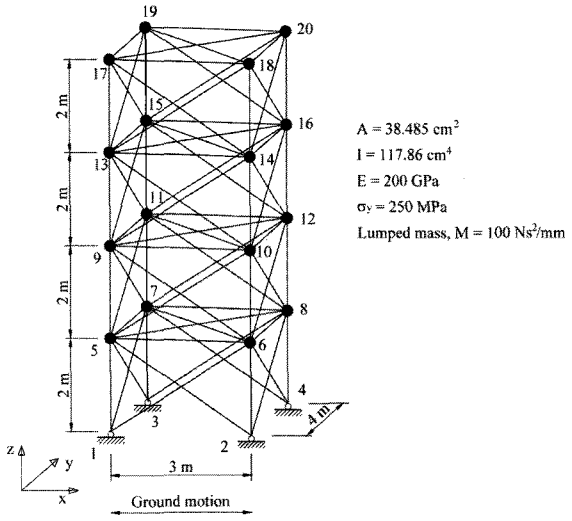

Fig. 5 Space truss

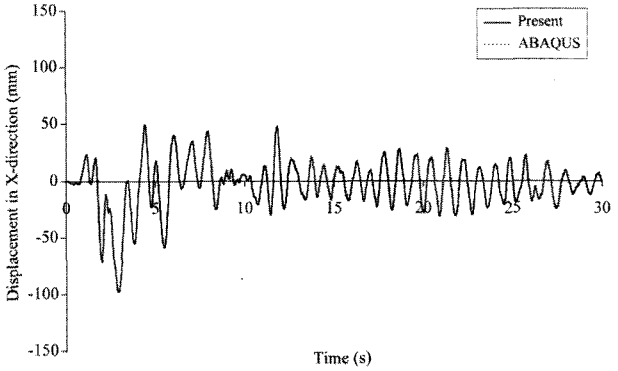

Fig. 6 Displacement response at the top of space truss under El Centro

As in the previous example, this one also indicates that the proposed program is able to accurately predict the seismic displacement, which is an important index for performance-based seismic design.

4.4 Two-story space frame under static loading

The space steel frame with rectangular sections is presented in Fig. 7 with its associated data. This structure was analyzed by De Souza(2000) using the force-based method with the fiber hinge model.

The analysis results of the proposed program are compared with those obtained by De Souza and ABAQUS as presented in Fig. 8. By using one element per member, the load-displacement curve obtained by the proposed program is found to be consistent with that given by De Souza. ABAQUS cannot predict accurately the nonlinear inelastic response of the space frame by using ten elements per member. The accuracy can only be seen when more

than fifty elements are used, and the load- displacement curve is then close to the result predicted by De Souza. It can be concluded that the proposed program can accurately predict the nonlinear inelastic behavior of the space frame by using only one element per member, while the ABAQUS program needs more than fifty elements to match the results of the proposed program.

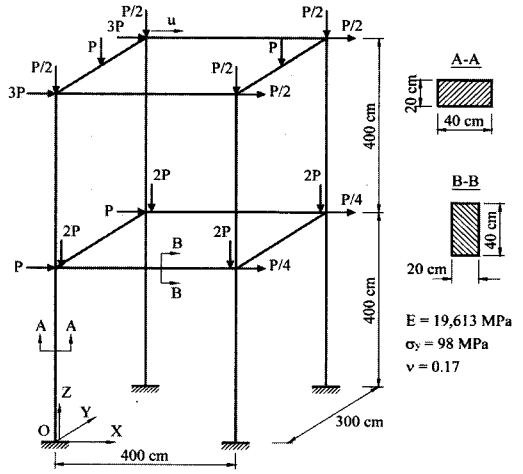

Fig. 7 Two-story space frame under static loading

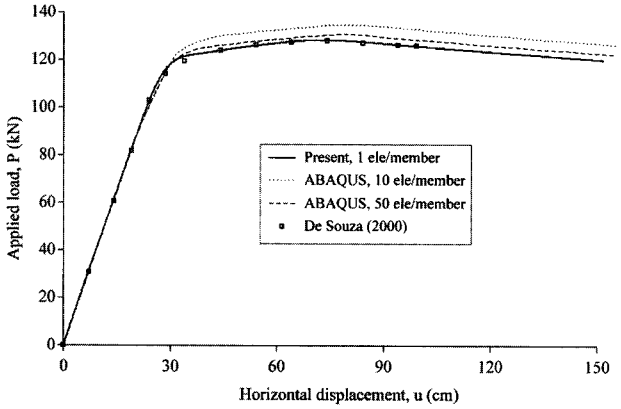

Fig. 8 Load-deflection curves of two-story space frame under static loading

5. Case study

A three-dimensional modeling of cable suspension bridge is shown in Fig. 9. The Young's modulus and yield stress of beam-column members are 200 GPa and 248 MPa, respectively, while the Young's modulus and yield stress of cable members are 165.5 GPa and 1,103 MPa, respectively. The weight per unit volume of the cable and beam-column members is 60.5 kN/m^3 and 76.82 kN/m^3, respectively. The purpose of this case study is to confirm that the proposed program can be used to predict accurately and efficiently nonlinear inelastic response of steel suspension bridge when compared to SAP2000.

The total loadings of the bridge consist of dead load, girder live load and earthquake load. The girder dead load is taken as 85 kN/m which is determined mainly by the own weight of the steel girder. The uniform live load applied to girder is 42.3 kN/m. The El Centro earthquake applied in the longitudinal direction of the bridge is scaled up by a factor of 2.5 to produce highly nonlinear inelastic behavior in this structure. For the finite element modeling, the main cable and hanger are modeled using one cable element per member in both proposed program and SAP2000. The cross beam, girder, and tower members are modeled using only one beam-column element per member in proposed program and five frame elements per member in SAP2000. A fiber

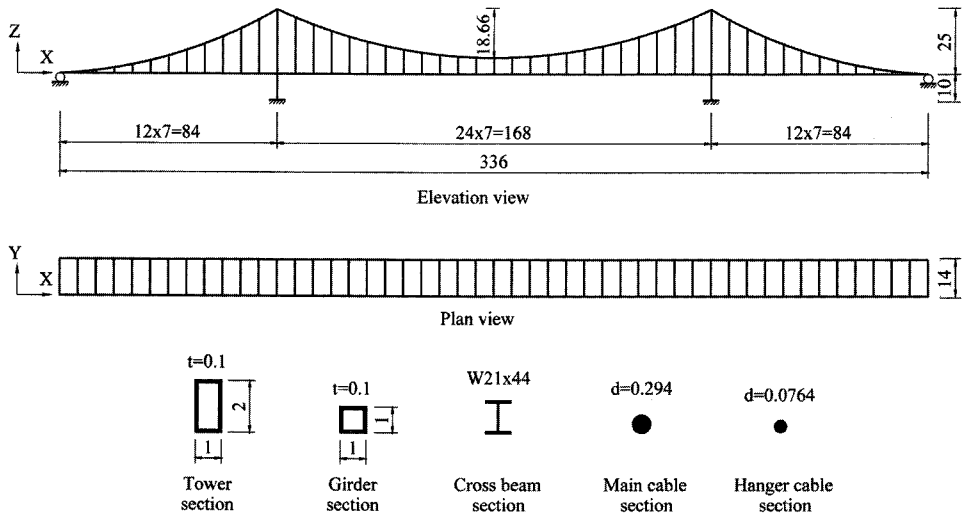

Fig. 9 Geometry and dimension of suspension bridge(unit : m)

P-M hinge model in which the cross-sections of girder and tower are divided into 220 fibers and 420 fibers, respectively, is employed to capture the inelastic behavior in SAP2000.

To investigate the ultimate load-carrying capacity and the behavior of suspension bridge, the analysis procedure can be divided into two steps. In the first step, initial shape analysis is carried out to determine the initial cable tension and deformed configuration of the bridge under the dead load. Once the first step is achieved, the load-displacement analysis is performed to evaluate the ultimate strength and behavior of the suspension bridge subjected to dead and live loadings. The load-displacement curves of the bridge predicted by the proposed program are compared well with those obtained by SAP2000 as shown in Fig. 10. Since the load-displacement curves are almost in straight lines before the first plastic hinge are developed, it implies that the effects of geometric nonlinearity of the bridge members, including the cable sag effect, are not significant in the early ultimate behavior of the bridge. The ultimate load factors of the bridge obtained by the proposed program and SAP2000 are 3.124 and 3.127, respectively. It can be seen that the difference between the ultimate load factors predicted by the proposed program and SAP2000 is less than 1%.

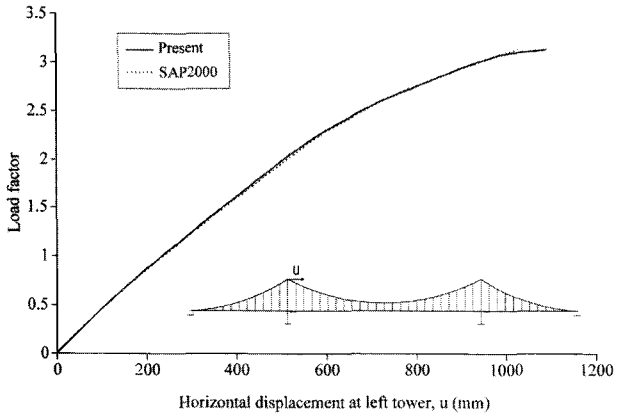

Fig. 10 Load-displacement curves of bridge under live load

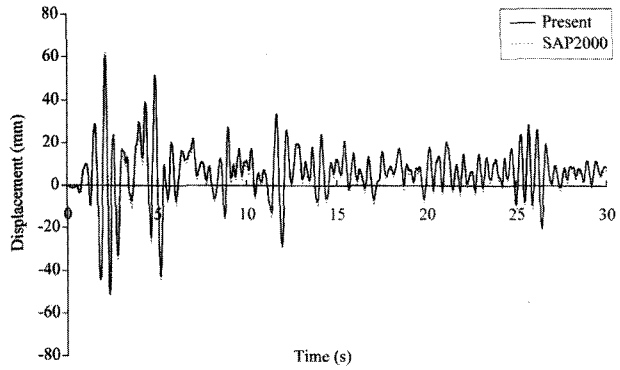

Fig. 11 Longitudinal inelastic response at the midspan of the suspension bridge

The longitudinal displacement response at the midspan of the bridge predicted by the proposed program is compared with those obtained by SAP2000 as shown in Fig. 11. It can be seen that the proposed program and SAP2000 give nearly identical results including the slight permanent shifts in displacement response due to inelastic behavior.

6. Conclusion

An advanced analysis program which can be used for nonlinear inelastic analysis of space steel structures is developed. The proposed program employs the stability functions and refined plastic hinge model for nonlinear inelastic analysis of space steel frames to minimize modeling and solution time. As shown in some numerical examples, the proposed program demonstrates the accuracy and the computational efficiency in predicting the nonlinear inelastic response of space steel structures. It can be concluded that the proposed software proves to be reliable and valuable for application in engineering design.

References

1. De Souza, R., 2000. Force-based finite element for large displacement inelastic analysis of frames. PhD Dissertation, Dept of Civil and Environmental Engineering, University of California at Berkeley
2. Heidari, A., and Salajegheh, E., 2006. Time history analysis of structures for earthquake loading by wavelet networks. Asian Journal of Civil Engineering(Building and Housing) 7, 155-168
3. Hill, C. D., Blandford, G. E., and Wang, S. T., 1989. Post-buckling analysis of steel space trusses. Journal of Structural Engineering 115, pp.900-919
4. Thai, H. T., and Kim, S. E., 2009. Practical advanced analysis software for nonlinear inelastic analysis of space steel structures. Advances in Engineering Software 40, pp.786-797
5. Yang, Y. B., and Kuo, S. R., 1994. Theory & analysis of nonlinear framed structures. Prentice-Hall Englewood Cliffs, NJ
6. Yang, Y. B., and Shieh, M. S., 1990. Solution method for nonlinear problems with multiple critical points. AIAA Journal 28, pp.2110-2116

[담당 : 노혁천, 편집위원]